Functional analysis of the GTPases EngA and YhbZ encoded by *Salmonella typhimurium*

HEATHER K. LAMB,[1] PAUL THOMPSON,[1] CATHERINE ELLIOTT,[1] IAN G. CHARLES,[2] JAMIE RICHARDS,[3] MICHAEL LOCKYER,[3] NICHOLAS WATKINS,[1] CHARLES NICHOLS,[4] DAVID K. STAMMERS,[4] CLIVE R. BAGSHAW,[5] ALAN COOPER,[6] AND ALASTAIR R. HAWKINS[1]

[1]Institute of Cell and Molecular Biosciences, Medical School, Newcastle University, Newcastle upon Tyne NE2 4HH, United Kingdom
[2]Wolfson Institute for Biomedical Research, University College London, London WC1E 6AU, United Kingdom
[3]Arrow Therapeutics, Britannia House, London SE1 1DA, United Kingdom
[4]Division of Structural Biology, Wellcome Trust Centre for Human Genetics, University of Oxford, Oxford OX3 7BN, Untied Kingdom
[5]Department of Biochemistry, University of Leicester, Leicester LE1 9HN, United Kingdom
[6]Department of Chemistry, University of Glasgow, Glasgow G12 8QQ, United Kingdom

(RECEIVED March 26, 2007; FINAL REVISION July 10, 2007; ACCEPTED August 20, 2007)

Abstract

The *S. typhimurium* genome encodes proteins, designated EngA and YhbZ, which have a high sequence identity with the GTPases EngA/Der and ObgE/CgtA$_E$ of *Escherichia coli*. The wild-type activity of the *E. coli* proteins is essential for normal ribosome maturation and cell viability. In order to characterize the potential involvement of the *Salmonella typhimurium* EngA and YhbZ proteins in ribosome biology, we used high stringency affinity chromatography experiments to identify strongly binding ribosomal partner proteins. A combination of biochemical and microcalorimetric analysis was then used to characterize these protein:protein interactions and quantify nucleotide binding affinities. These experiments show that YhbZ specifically interacts with the pseudouridine synthase RluD ($K_D = 2$ μM and 1:1 stoichiometry), and we show for the first time that EngA can interact with the ribosomal structural protein S7. Thermodynamic analysis shows both EngA and YhbZ bind GDP with a higher affinity than GTP (20-fold difference for EngA and 3.8-fold for YhbZ), and that the two nucleotide binding sites in EngA show a 5.3-fold difference in affinity for GDP. We report a fluorescence assay for nucleotide binding to EngA and YhbZ, which is suitable for identifying inhibitors specific for this ligand-binding site, which would potentially inhibit their biological functions. The interactions of YhbZ with ribosome structural proteins that we identify may demonstrate a previously unreported additional function for this class of GTPase: that of ensuring delivery of rRNA modifying enzymes to the appropriate region of the ribosome.

Keywords: EngA; YhbZ; RluD; microcalorimetry; ribosome

Supplemental material: see www.proteinscience.org

The functions of many GTPases are closely associated with normal ribosome maturation in both prokaryotes and eukaryotes, and are therefore of central importance to the viability of the cell (Caldon and March 2003; Brown 2005; Dutca and Culver 2005). Now that structures for the prokaryotic ribosome are available (Wimberly et al.

Reprint requests to: Alastair R. Hawkins, Institute of Cell and Molecular Biosciences, Medical School, Newcastle University, Framlington Place, Newcastle upon Tyne NE2 4HH, UK; e-mail a.r.hawkins@ncl.ac.uk; fax +44 (0)-191-2227673.

Article published online ahead of print. Article and publication date are at http://www.proteinscience.org/cgi/doi/10.1110/ps.072900907.

2000; Schuwirth et al. 2005), interest in targeting such organelles with novel antibacterials has been stimulated (Poehlsgaard and Douthwaite 2005). In this respect the view has been expressed that, because of their association with the ribosome, prokaryotic GTPases should be considered as a new target for antibacterial drugs (Comartin and Brown 2006).

In *Salmonella typhimurium* the genes *engA* and *yhbZ* encode the GTPases EngA (called Der and EngA in *Escherichia coli*) and YhbZ (called ObgE and $CgtA_E$ in *E. coli*) (Caldon et al. 2001). The structure of the *Bacillus subtilis* YhbZ ortholog is known and is typical of this class of GTPase in that it has a single GTP-binding domain (Buglino et al. 2002; Wittinghofer 2002). EngA, on the other hand, is unique among prokaryotic and eukaryotic GTPases as it has two adjacent GTPase domains (Robinson et al. 2002). In *E. coli* mutations in the *engA* ortholog EngA/Der cause cells to elongate into filaments and block chromosome segregation (Hwang and Inouye 2001). Mutations in homologs of the *obgE* gene cause pleiotropic defects in various species including effects on rRNA processing, ribosomal protein levels, ribosomal protein modification, and consequently the levels of the mature 70S ribosome (Sato et al. 2005). In *E. coli* the growth rate correlates with the amount of ObgE/$CgtA_E$ protein. Cosedimentation experiments suggest that *E. coli* ObgE binds to the 30S and 50S subunits of the ribosome, and pulldown experiments with 6His-tagged protein suggest that it associates with several specific ribosomal proteins (Sato et al. 2005). The GTPase ObgE/$CgtA_E$ in *E. coli* is involved in the late steps of large ribosome assembly (Jiang et al. 2006); however, despite these important observations, the precise functions of prokaryotic GTPases are not clearly understood. Eukaryotes, on the other hand, have large families of GTPases that are important regulators of membrane signal pathways (Caldon and March 2003).

The gene *rrmJ* of *E. coli* encodes a heat-induced rRNA methyltransferase that is responsible for methylating position U2552 of 23S rRNA in intact 50S ribosomal subunits. In-frame deletions of *rrmJ* cause disruption of ribosome biogenesis with an accumulation of ribosomal subunits at the expense of the functional 70S mature ribosome. In an experiment using this deletion strain to screen for genes whose overexpression could restore its severe growth defect, no methylases were detected. Surprisingly, however, the genes *engA* and *yhbZ* were identified in this screen, suggesting an association between rRNA methylation and GTPase activity (Tan et al. 2002). The molecular mechanism by which the overexpression of the *yhbZ* and *engA* genes relieves the severe growth defect of *rrmJ* null mutants is not clear. Analysis of the overexpressing strains showed that the 23S rRNA still lacked the highly conserved Um2552 modification, showing that the relief of the severe growth defect was not by YhbZ or EngA directly supplying the missing methyltransferase activity (Tan et al. 2002). It is not known if the GTPase activity of YhbZ and EngA is required for their ability to ameliorate the growth defect of *rrmJ* null mutants, and it may be that they recruit some other protein(s) that is/are responsible for the effect.

We report here the results of stringent affinity chromatography and microcalorimetry experiments designed to understand more closely the biological role of EngA and YhbZ in *S. typhimurium* through an analysis of their protein:protein and protein:ligand interactions. We show that EngA interacts with the 30S subunit ribosomal proteins S7 and S9 and that YhbZ interacts with S3, S5, and S9, thereby suggesting a mechanism for targeting these essential GTPases to the head region of the 16S rRNA. Significantly, we find that YhbZ also specifically interacts with the rRNA pseudouridylate synthase, RluD, thereby providing a potential molecular mechanism for targeting this important rRNA-modifying enzyme to its site of action. This specific interaction of YhbZ with RluD may reveal an additional function for this GTPase that is required for the specific targeting of rRNA-modifying enzymes to their site of action. Given the biological importance of EngA and YhbZ and the current interest in targeting their biological activity with new antibacterials, we report a simple fluorescence assay for nucleotide binding. This assay can be adapted to a microtiter plate format for a high-throughput screen designed to identify inhibitor molecules specific for the nucleotide-binding site. Such compounds would allow the targeting of the biological activity of these proteins.

Results

Identification of partner proteins for EngA and YhbZ

In order to understand the relationship between *S. typhimurium* EngA, YhbZ, and the biology of the ribosomes we undertook a search for ribosome-associated partner proteins. Previous pulldown approaches have used recombinant 6His-tagged protein expression followed by loading the resulting *E. coli* whole-cell lysates onto Ni-NTA resin. Proteins are recovered by imidazole elution (Sato et al. 2005) and specific protein binding is characterized following comparison with the ''control'' profile of proteins recovered from *E .coli* expressing the 6His-tag alone (Sato et al. 2005). We covalently linked around 300 mg of purified EngA or YhbZ to 25 mL of NHS-activated Sepharose 4B and used these resins as affinity columns to isolate binding proteins from a sonicated cell-free extract of *S. typhimurium* as described in Materials and Methods. In overview, cell-free *S. typhimurium* extracts, incubated previously with RNase to disrupt protein:RNA

interactions, were loaded onto the affinity columns which were then washed with 10-column volumes of buffer and eluted with a 20-column volume 0–1.0 M NaCl gradient in buffer collecting 5-mL fractions. The rationale for this procedure was to fractionate the binding proteins according to their relative affinities for the target protein. We chose to select partner-binding proteins that required at least 0.15 M NaCl to elute them from the affinity columns. In this way the chances of recovering proteins that were binding nonspecifically to the bait proteins was minimized. SDS-PAGE was then used to locate eluted proteins that were subsequently excised from the gel and their identities assigned by peptide mass fingerprinting as described in Materials and Methods. Table 1 lists the proteins that were identified by this process and shows that ribosome-associated proteins are the most abundant class. The protein assignments shown in Table 1 have a probability of being a random match of $P < 0.05$, and in each case the predicted M_r of the assigned protein matches that experimentally observed, indicating that the assignments are therefore likely to be correct. This analysis (see Table 1) showed that EngA and YhbZ bound the ribosomal structural protein S9 and that additionally EngA bound S7. This is the first time these interactions have been reported; however, *E. coli* ObgE has been reported to bind to the ribosomal S3/4/5/13/14/ and 16 proteins (Sato et al. 2005). To determine whether S9 has a nonspecific affinity for any protein attached to the NHS-Sepharose column, a control experiment was carried out with the YegS protein of *S. typhimurium*. YegS is a putative lipid kinase homologous to eukaryotic sphingosine and diacylglycerol kinases, and therefore not involved in ribosome maturation. Additionally, YegS will be strongly negatively charged (pI 4.7), and thus a good test for nonspecific binding of the positively charged S7/S9 proteins (pIs > 10) under our experimental conditions, compared to EngA and YhbZ (pIs 5.8 and 4.8). No binding of S9 to YegS was detected (although binding to OmpH was identified), supporting the hypothesis that the interaction of S9 with YhbZ and S7 with EngA is likely to be specific. Interestingly, YhbZ was found to bind to the pseudouridine synthase RluD, independently identifying a previously observed, but unverified, interaction reported in the Supplemental material of an *E. coli* protein network experiment (Butland et al. 2005). The possible interactions between YhbZ and the hypothetical periplasmic ATP-binding protein encoded by *yncE*, and the pyrroline-5-carboxylate reductase encoded by *proC* were not further studied, as the purpose of this study was to focus on the relationship between *S. typhimurium* EngA, YhbZ, and the biology of the ribosomes.

Thermodynamic and biochemical analysis of the interactions between YhbZ and RluD/S9

We purified the RluD and S9 proteins in bulk and carried out a thermodynamic analysis of their interactions with YhbZ. RluD at 350–400 μM was titrated into YhbZ in the ITC cell in the range of 36–50 μM, and an exothermic binding thermogram, adequately described by a single-site binding model, was observed. Typical data are shown in Figure 1 and Table 2, and show that YhbZ and RluD interact with a K_D of ~2.1 μM and an approximate 1:1 stoichiometry. These experiments were repeated in the presence of saturating concentrations (85 μM) of GDP or GTP (see below), but there was no effect on the interaction of YhbZ with RluD (data not shown). Similarly, there was no effect on the interaction between YhbZ and RluD in the presence of 100 μM of guanosine-[β,γ-imido] triphosphate, a nonhydrolysable analog of GTP.

The interaction with S9 was more problematic to study, as the S9 protein proved difficult to purify in bulk and had a low solubility. This low solubility required the S9 to be in the ITC cell at the relatively low concentration of

Table 1. *Ribosome-associated partner proteins for EngA and YhbZ*

Target protein	Gene designation	Protein function	MASCOT threshold score for $p \leq 0.05$	MASCOT score	Sequence coverage (%)
YhbZ	*rluD*	rRNA pseudouridylate synthase	76	121	63
YhbZ	*rpsC*	30S ribosomal protein S3	69	152	51
YhbZ	*rspE*	30S ribosomal protein S5	59	64	66
YhbZ	*rpsI*	30S ribosomal protein S9	56	59	58
EngA	*rpsG*	30S ribosomal protein S7	76	104	54
EngA	*rpsI*	30S ribosomal protein S9	56	58	45
YhbZ	*yncE*	Hypothetical periplasmic ATP-binding protein	76	185	48
YhbZ	*proC*	Pyrroline-5-carboxylate reductase	69	76	24

Ribosome-associated partner proteins for EngA and YhbZ identified by high stringency pulldown and peptide mass fingerprinting experiments are shown. The MASCOT score is a probability-based Mowse score where p is the probability that the observed match is a random event using a significance threshold of $p < 0.05$.

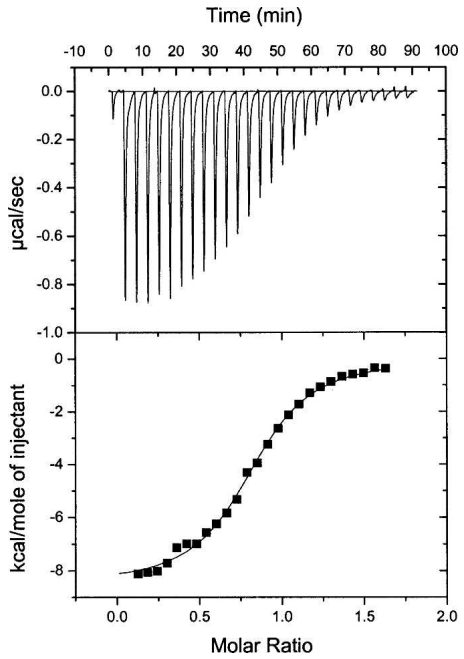

Figure 1. Typical ITC data for the exothermic binding of RluD to YhbZ. The *upper* panel shows heat change upon injection (1 × 2 μL and 24 × 10 μL) of 396 μM RluD into the calorimetric cell (1.4 mL) containing YhbZ (49 μM). Heat pulses in the absence of YhbZ were negligible. The *lower* panel shows integrated heat pulses, normalized per mol of injectant, showing a differential binding curve that is adequately described by a 1:1 binding model.

~25 μM and YhbZ in the injector in the range of 240–320 μM. The titration of YhbZ into S9 is associated with protein precipitation and a typical thermogram, fitted to a single-site binding model and showing an exothermic interaction, is shown in Figure 2. It is likely that the interaction of YhbZ and S9 is complex, with aggregation following the initial binding reaction that eventually becomes irreversible leading to precipitation. Given these considerations it is therefore not possible to derive accurate K_D measurements or stoichiometries from the data shown in Figure 2; however, they do confirm, qualitatively, that YhbZ and S9 interact with one another.

Thermodynamic and biochemical analysis of the interactions between EngA and S7/S9

When EngA was titrated into S9 at either 5°C or 25°C, the accompanying heat exchanges were small compared to the background heat of dilution. Consequently, ITC was unable to confirm the interaction of these two proteins seen in the pulldown experiments.

S7 (~248 μM) was injected into EngA (~32 μM) in the microcalorimeter cell, and a thermogram showing exothermic binding was observed. Similar to the YhbZ/S9 pairing, the interaction between EngA and S7 was associated with protein precipitation. A typical thermogram fitted to a single-site model is shown in Figure 3, and demonstrates in a qualitative manner that EngA and S7 interact with one another. We wished to investigate the possibility that the presence of GDP may affect the interaction between EngA and S7. However, when the concentration of GDP or GTP in the solution of S7 was 1 mM, mixing was again accompanied by protein precipitation.

Thermodynamic and enzymatic analysis of nucleotide binding to EngA and YhbZ

The known structures of EngA from *Thermotoga maritima* and the ortholog YphC from *B. subtilis* (Muench et al. 2006) imply that the *S. typhimurium* EngA will have two nucleotide-binding sites. Both nucleotide-binding domains in the *E. coli* EngA have been shown to be required for wild-type cellular activity (Bharat et al. 2006); however, inactivation of the C-terminal domain of the *T. maritima* enzyme does not reduce its overall GTPase activity (Robinson et al. 2002). When GTP was titrated into *S. typhimurium* EngA in the presence of Mg^{2+}, the heat exchanges observed did not vary over the length of the titration and could not be fitted to any binding model. These uniform heat exchanges are most simply interpreted as being associated with GTPase activity. In order to test this hypothesis, the experiments were repeated in the absence of Mg^{2+} and the uniform heat exchanges were replaced with titration curves consistent with two binding sites. One site showed

Table 2. *Thermodynamic parameters for binding of GTP, GDP, and RluD to YhbZ determined by ITC at 25°C*

Ligand tested	[Ligand] in syringe	[YhbZ] in cell	n	Average $K_{D(app)}$ μM	Average ΔH_{obs} kcal mol^{-1}	Average ΔS^0 cal K^{-1} mol^{-1}	c
GTP binding to YhbZ	0.5 mM GTP	51 μM	0.33 ± 0.1	6.5 ± 1.8	−15.5 ± 0.2	−28.3 ± 7.5	2.8 ± 0.9
GDP binding to YhbZ	0.5 mM GDP	51 μM	0.30 ± 0.1	1.7 ± 0.1	−13.3 ± 0.2	−18.8 ± 3.2	10.3 ± 0.8
RluD binding to YhbZ	396 μM RluD	49 μM	0.84 ± 0.1	2.1 ± 0.2	-8.4 ± 0.2	-2.2 ± 0.8	19.4 ± 2.6

The binding of GTP, GDP, and RluD to YhbZ was measured in 50 mM KPO_4, pH 7.2, 1 mM DTT, 1 mM $MgCl_2$ by ITC. The concentration of protein and ligands are shown in the table and the data were fitted to a single-site binding model. Shown are the values for *n*, the stoichiometry of binding; $K_{D(app)}$, the apparent equilibrium dissociation constant; ΔH_{obs}, the observed entropy change for single-site binding; and ΔS^0, the standard entropy change for single-site binding. Each value is the average of three repeat experiments and the standard deviations ± are shown. The *c* values fall within the range of 1–1000, which allows the isotherms to be accurately deconvoluted with reasonable confidence to derive the *K* values (Wiseman et al. 1989).

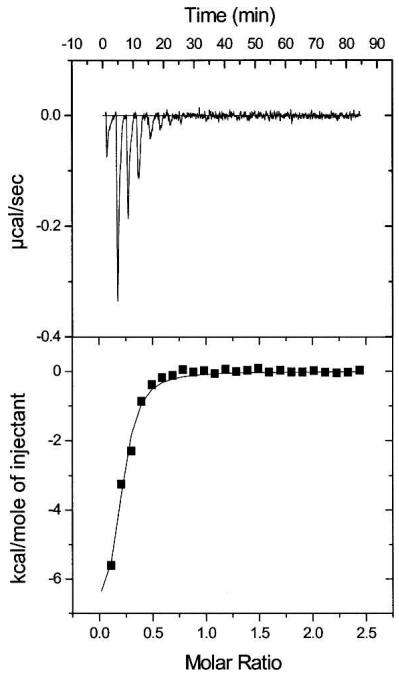

Figure 2. Typical ITC data for the exothermic binding of YhbZ to S9. The *upper* panel shows heat change upon injection (1 × 2 µL and 24 × 10 µL) of 320 µM YhbZ into the calorimetric cell (1.4 mL) containing S9 (24 µM). Heat pulses in the absence of S9 were negligible. The *lower* panel shows integrated heat pulses, normalized per mol of injectant, showing a differential binding curve that is fitted to a 1:1 binding model.

endothermic binding and the other exothermic binding. Typical data summarizing the associated thermodynamic parameters for GDP and GTP binding (done in the absence of Mg^{2+} to allow a direct comparison) are shown in Table 3, and Figure 4 shows a typical binding isotherm, adequately described by a two-site sequential binding model, for the binding of GDP to EngA. The data in Table 3 shows that the affinity of the weakest site for GTP is so low that it cannot be measured by this technique.

The two binding sites within EngA identified by thermodynamic analysis showed endothermic binding to the tightest binding site and exothermic to the weakest. The difference in the affinity of the two binding sites for GDP is modest at around fivefold, whereas the difference in affinity for GTP is marked. The ITC measurements show that the site with the highest affinity for GTP has a K_D of ~12.7 µM, and that the affinity of the second site is too weak to measure by this technique. ITC can usually reliably detect binding up to 10^3 M^{-1} (O'Brien et al. 2000); therefore, the K_D for the second site is likely to be in excess of 100 µM, putting it at least an order of magnitude greater than the first site. This difference in affinity means that in quantitative terms the contribution of the weak binding site to the overall turnover number of the enzyme is likely to be low at physiological concentrations of nucleotide. The structure of the *T. maritima* EngA ortholog Der shows that it has two nucleotide-binding sites, one near the N terminus (GD1) and one near the C terminus (GD2) (Robinson et al. 2002). Biochemical analysis of the *T. maritima* ortholog shows that inactivation of the GD2 site does not reduce the overall GTPase activity of the protein, whereas inactivation of GD1 does (Robinson et al. 2002). In contrast, mutant substitutions in either domain of *E. coli* EngA have a phenotypic effect, suggesting that both domains are important for viability and function (Bharat et al. 2006). When viewed in light of the structural data for the *T. maritima* ortholog (Robinson et al. 2002), our data imply that the strong binding of GTP to the single site we see in these ITC experiments with EngA identifies it as the N-terminal site. If, as is likely, there is a similar disparity in the K_D for the two sites in the *T. maritima* enzyme, this provides a molecular explanation for the observation that inactivation of the C-terminal nucleotide-binding site in *T. maritima* EngA does not reduce the overall GTPase activity of the enzyme.

Based on the structure of the protein from *B. subtilis* (Buglino et al. 2002), YhbZ is predicted to contain a single nucleotide-binding site. In order to investigate the interaction between YhbZ and GDP/GTP in more detail by ITC, we titrated GTP or GDP (0.5 mM) into YhbZ (50 µM) in the presence of Mg^{2+}. Inspection of the thermodynamic parameters shown in Table 2 demonstrates that

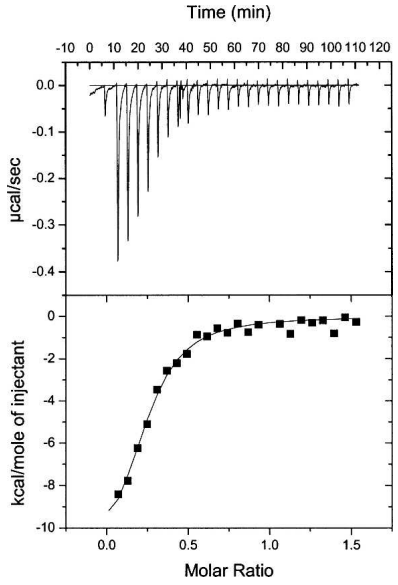

Figure 3. Typical ITC data for the exothermic binding of S7 to EngA. The *upper* panel shows heat change upon injection (1 × 2 µL and 24 × 10 µL) of 248 µM S7 into the calorimetric cell (1.4 mL) containing EngA (30 µM). Heat pulses in the absence of EngA were negligible. The *lower* panel shows integrated heat pulses, normalized per mol of injectant, showing a differential binding curve that is fitted to a 1:1 binding model.

Table 3. *Thermodynamic parameters for binding of GTP and GDP to EngA determined by ITC at 25°C*

Ligand tested	[Ligand] in syringe	[EngA] in cell	Average $K_{D(app)}$ μM	Average ΔH_{obs} kcal mol^{-1}	Average ΔS^0 cal K^{-1} mol^{-1}	c
GTP binding to EngA high affinity site	3 mM GTP	50 μM	12.7 ± 1	2.8 ± 0.5	30.6 ± 1	4.1 ± 1
GTP binding to EngA low affinity site	3 mM GTP	50 μM	NA[a]	NA[a]	NA[a]	<1
GDP binding to EngA high affinity site	3 mM GDP	50 μM	0.6 ± 0.1	1.5 ± 0.2	33.4 ± 0.8	87 ± 17
GDP binding to EngA low affinity site	3 mM GDP	50 μM	3.2 ± 0.4	−2.6 ± 0.3	16.3 ± 0.7	15.7 ± 2.5

The binding of GTP and GDP to EngA was measured in 50 mM KPO_4, pH 7.2, 1 mM DTT by ITC. The concentration of protein and ligands are shown in the table, and the data were fitted to a two-site sequential-binding model. Shown are the values for $K_{D(app)}$, the apparent equilibrium dissociation constant; ΔH_{obs}, the observed entropy change for each site binding; and ΔS^0, the standard entropy change for each site binding. Each value is the average of three repeat experiments and the standard deviations ± are shown. The *c* values fell within the range of 1–1000 (Wiseman et al. 1989) allowing the isotherms to be deconvoluted with reasonable confidence to derive the *K* values. The *c* value for GTP binding to site two was below 1 and could not be used to derive the *K* values.

[a]NA = not applicable because the *c* value is <1.

the K_D for GDP binding is similar to that for the weaker of the two binding sites in EngA. However, the stoichiometry of binding for GDP and GTP to YhbZ (Table 2) is ~0.33 rather than the expected 1:1 ratio predicted from the structure of the enzyme. One possible cause of a deviation from a 1:1 predicted stoichiometry is if the calculations use measurements of heat exchange that do not fully reach the baseline between injections. To obviate this possible problem we calculated the results from ITC data sets that had differing intervals between injections, but the stoichiometry was not significantly increased. Figure 5 shows a typical thermogram that had 450-s intervals between injections, ensuring that after each injection the signal had reached the baseline.

Another potential explanation for the deviation from a 1:1 stoichiometry is that the purified YhbZ had substantial occupation of its nucleotide-binding sites at the end of the purification procedure. However, typical preparations of *S. typhimurium* YhbZ had A_{280}/A_{260} ratios of ~1.6, implying that the protein had very little nucleotide contamination, and therefore, that the GTP-binding site did not have substantial occupancy with either GTP or GDP at the start of the ITC experiments. Nevertheless, we cannot rule out the possibility that YhbZ purified this way has significant occupancy of the GDP-binding site with a non-nucleotide ligand. Taking all the data as a whole, the simplest explanation for the deviation from the predicted 1:1 stoichiometry is that a large proportion of the YhbZ molecules (around 60%) are unable to bind nucleotides. This may be the result of inactivation during purification. It is relevant to note that a similar but less extreme effect is seen with the homologous Obg protein of *B. subtilis*. In this case, it was reported that after purification, 20% of the Obg was unable to bind the nucleotide (Welsh et al. 1994). However, the same population of YhbZ molecules is able to bind RluD with a stoichiometry of 0.84:1, closely approaching 1:1 (see above). The effect is thus limited to the nucleotide-binding domain, and would be equally consistent with an extreme negative cooperativity operating between subunits of a higher oligomeric state (e.g., 100% activity with a trimer and one-third of sites' reactivity). In this regard it is relevant to note that the apparent native M_r of the majority of the YhbZ determined by size exclusion chromatography is ~66 kDa. Analysis by SDS-PAGE showed that the YhbZ we purified has a

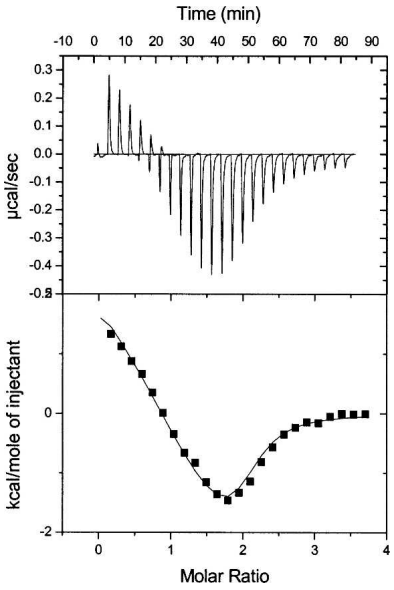

Figure 4. Typical ITC data for the binding of GDP to EngA. The *upper* panel shows heat change upon injection (1 × 2 μL and 24 × 10 μL) of 3 mM GDP into the calorimetric cell (1.4 mL) containing EngA (50 μM). Heat pulses in the absence of EngA were negligible. The *lower* panel shows integrated heat pulses, normalized per mol of injectant, showing a differential binding curve that is adequately described by a two-site sequential-binding model.

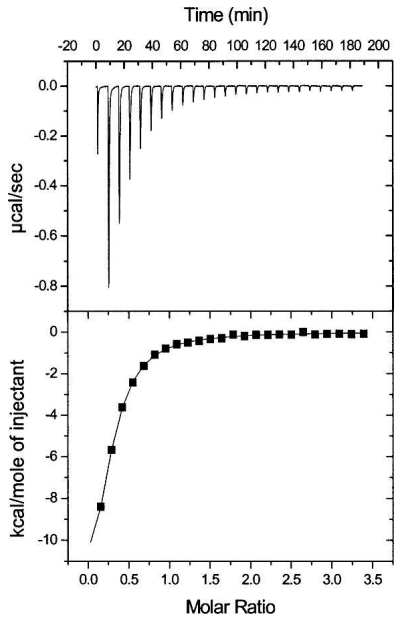

Figure 5. Typical ITC data for the exothermic binding of GDP to YhbZ. The *upper* panel shows heat change upon injection (1 × 2 μL and 24 × 10 μL) of 0.5 mM GDP into the calorimetric cell (1.4 mL) containing YhbZ (51 μM); the spacing between injections was 450 s. Heat pulses in the absence of YhbZ were negligible. The *lower* panel shows integrated heat pulses, normalized per mol of injectant, showing a differential binding curve that is adequately described by a 1:1 binding model.

migration consistent with its predicted M_r of 43.1 kDa and analysis by mass spectrometry (data not shown) gave a value of 43.1 kDa (±0.1%). The apparent value of 66 kDa for the M_r of native YhbZ is difficult to reconcile with the values obtained by SDS-PAGE and mass spectrometry; however, taken as a whole, the data are consistent with the bulk of YhbZ being monomeric. This interpretation is not consistent with negative cooperativity. However, there is a small but nonetheless significant amount of aggregated material with a shallow peak at an estimated M_r of ~160 kDa. The additional aggregated material present may not be biologically active, and could explain the small deviation from a 1:1 stoichiometry for the YhbZ:RluD interaction. The reason for the deviation from a 1:1 stoichiometry is thus likely to be due to inactivation of the nucleotide-binding site during the purification of the protein. This means that the active fraction of the protein is much less than the concentration used in the calculation of the stoichiometry and the thermodynamic parameters. If the data for YhbZ shown in Table 2 are recalculated, assuming an active protein fraction amounting to 33% of the total, the calculated stoichiometry is 1:1. The recalculated K_D for GDP is 1.4 μM, an ~18% change, and for GTP is 6.4 μM, an ~3% change. These calculations imply that the K_D values we report are likely to be accurate even though there is uncertainty in the stoichiometry. We determined the K_D for GDP and GTP binding to YhbZ in the presence of saturating concentrations of RluD. The results (data not shown) demonstrated that the presence of RluD had no effect on the K_D for either GDP or GTP. Additionally, we assayed the GTPase activity of YhbZ in the presence of increasing quantities of RluD and found that the activity was unchanged (data not shown).

Using GTP at 0.5 mM as the substrate in the presence of an excess of Mg^{2+} (5 mM) we initiated analyses of the turnover numbers for YhbZ and EngA, as described in Materials and Methods. The turnover number for EngA was determined to be 0.43 min^{-1} and for YhbZ 0.06 min^{-1} at 30°C, low values typical of this class of enzyme. The calculated turnover number of YhbZ is ~10-fold higher than that of the *B. subtilis* Obg GTPase (0.006 min^{-1}) (Sullivan et al. 2000); however, it may be an underestimate due to the potential presence of a substantial proportion of protein unable to bind nucleotides.

Development of an assay for nucleotide-binding site inhibitors of EngA and YhbZ

The *engA* and *yhbZ* genes of *S. typhimurium* are indispensable for growth under laboratory conditions (Knuth et al. 2004); consequently, the EngA and YhbZ proteins are potential targets for drug development if a simple assay could be designed. The data presented above show that EngA and YhbZ bind GDP and GTP in the micromolar range, thereby opening the possibility for an assay which monitors the displacement of the nucleotide from its binding sites. YhbZ has been shown to bind to *N*-methyl-3′-*O*-anthranoyl (mant)-GDP and -GTP (Wout et al. 2004); however, to develop a displacement assay we used BODIPY FL GDP because the BODIPY group is attached to the ribose moiety, and therefore, according to the crystal structure of the *T. maritima* protein (Robinson et al. 2002), it will be solvent exposed when bound and unlikely to perturb the K_D by any significant degree. Figure 6A shows the increase in fluorescence when EngA in the range of 0–5 μM is titrated into a buffer containing 100 nM BODIPY FL GDP but lacking Mg^{2+}. This was done so that the data in Figure 6 can be directly compared with the data in Figure 4. When analyzed for a single class of sites, the best fit yielded a K_D of 0.65 μM. If a second class of weaker sites were present they would not be revealed in this assay because the concentration of the BODIPY FL GDP is less than the K_D of the first site. Figure 6B–C shows that GDP and GTP can displace the BODIPY FL GDP from EngA in a buffer lacking Mg^{2+}. Analysis of the data in terms of competition for a single (high affinity) site yields a K_D of 1.1 μM for GDP and 21 μM for GTP. These values agree with the K_Ds determined by ITC data to within a factor of 2.

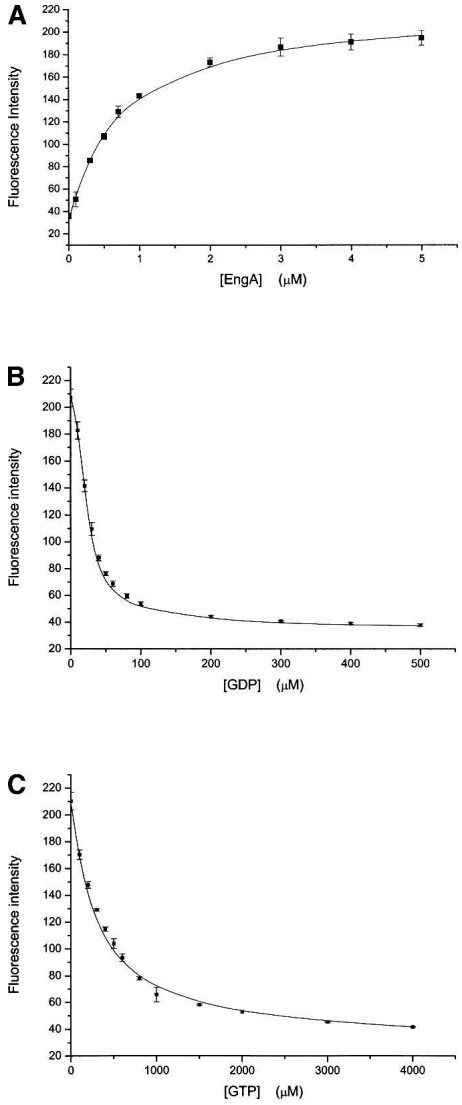

Figure 6. Analysis of EngA binding to BODIPY FL GDP determined by fluorescence assay. (*A*) The direct titration of 100 nM Bodipy FL GDP with increasing concentrations of EngA. (*B*) Competition assay of EngA (9 μM) binding to 100 nM Bodipy FL GDP in the presence of increasing amounts of unlabeled GDP. (*C*) Competition assay of EngA (9 μM) binding to 100 nM Bodipy FL GDP in the presence of increasing amounts of unlabeled GTP. The error bars in each case show the standard deviation of three replicates.

The fluorescence data are insufficient to model two classes of sites uniquely, but force fitting the curves to two classes of site with the K_D values determined by ITC show that the data are compatible with this model and indeed showed a 50% reduction in the standard error of the fit compared with a single class of site. When these experiments were repeated in the presence of 1 mM Mg^{2+}, the binding of BODIPY FL GDP and GDP was weakened approximately twofold, but there was no effect on GTP (data not shown). Similar fluorescence changes were observed when YhbZ was used (data not shown), and as this assay is compatible for use with microtitre plates, it can be simply developed to screen for inhibitors of EngA and YhbZ that compete for the nucleotide binding site.

Discussion

The EchoBase post-genomic database and reports of protein network studies (Butland et al. 2005; Misra et al. 2005) are a good source for identifying potential protein:protein interactions. Many of the reported interactions between these partner proteins have not been verified, and there is no quantitative information relating to the affinity or the stoichiometry of the various proposed interactions. We chose to screen for ribosome-associated partner binding proteins for YhbZ and EngA by affinity chromatography and subsequently used microcalorimetry as an additional independent technique to verify some of the interactions detected. This combined analysis (see Table 1; Figs. 2, 3) showed that YhbZ bound the ribosomal structural protein S9 and that EngA bound S7. This is the first time these interactions have been reported; however, *E. coli* ObgE has been reported to bind to the ribosomal S3/4/5/13/14/ and 16 proteins (Sato et al. 2005). Additionally, *E. coli* $CgtA_E$ and Der have been shown to be associated with the mature 50S ribosomal subunit (Hwang and Inouye 2006; Jiang et al. 2006). It is worthy of note that the experiments we report here did not identify an interaction of EngA with any 50S ribosome component. This may reflect the fact that we recovered proteins purified from cell-free extracts of *S. typhimurium* that had been incubated in the presence of RNase I and thus lacked mature ribosomes. These proteins were eluted from the affinity columns with buffer containing >150 mM NaCl, and it is possible that this strategy screened out potential interactions with 50S ribosomal proteins. The observation that we can detect interactions of EngA and YhbZ with small subunit structural proteins may indicate that these GTPases interact with both small and large ribosome subunits at different times in the maturation of the complete ribosome.

The binding of YhbZ with S9 and EngA with S7 was complex and led to aggregation, which became irreversible, thereby causing precipitation. The reason for the observed precipitation may be due to the likelihood that S7 and S9 only interact in vivo with YhbZ and EngA when they are already bound to the 30S ribosome subunit. In this environment they will be orientated in a specific manner on the rRNA scaffold, whereas in solution they will be able to interact with a much greater degree of freedom. In this latter instance additional interactions between the proteins may occur stimulating the formation of insoluble aggregates. Taken as a whole, the ITC analysis of protein binding confirmed the specificity of

the various interactions implied by the affinity chromatography experiments.

GTPases are often referred to as molecular switch proteins because they hydrolyze GTP in a cyclical manner, alternating between active and inactive states with GTP hydrolysis associated with an effect being generated on the target of the GTPase (Caldon et al. 2001). Additionally, some GTPases interact with many different effectors and targets and, in that way, can coordinate cellular responses (Caldon et al. 2001). However, the interaction of RluD with YhbZ did not stimulate the GTPase activity of YhbZ, and the presence of GTP had no effect on the K_D for binding of these two proteins. The latter of these observations is consistent with the structural analysis of the orthologous *B. subtilis* ObgE protein that shows the binding of nucleotide did not cause any significant conformational changes (Buglino et al. 2002). It may be that the GTPase activity of YhbZ is only stimulated in the presence of RluD when the stem–loop structure of helix 69 of the 23S rRNA that forms the substrate for RluD is present.

The structure of the prokaryotic ribosome has been elucidated from which the topography of the structural proteins has been determined (see Fig. 7) (Wimberly et al. 2000; Schuwirth et al. 2005). The 30S subunit shape is largely determined by the RNA component. In the canonical front view from the 50S, the tertiary fold of 16S RNA shows a head with a beak pointing leftward, the body with the shoulder at the top left and the spur at the lower left, and the platform at top right (Wimberly et al. 2000). The S7 protein binds to the head region of the 30S ribosomal 16S rRNA and facilitates the association of S9 with the assembling 30S subunits. These proteins are therefore close to the interface between the 50S and 30S subunits and the peptidyl transfer center (PTC) that carries out the peptide elongation step (Wimberly et al. 2000; Schuwirth et al. 2005). In vivo RluD (a pseudouridine synthase) is responsible for the formation of Ψ1911, Ψ1915, and Ψ1917 on the stem loop structure of helix 69 located in domain IV of the 23S rRNA located in the 50S subunit (Spedaliere et al. 2004; Gutgsell et al. 2005; Liiv et al. 2005). This helix forms part of the PTA pocket, and is close to the head region of the 30S subunit, bringing it close to the S3, S5, and S9 proteins (Wimberly et al. 2000; Schuwirth et al. 2005).

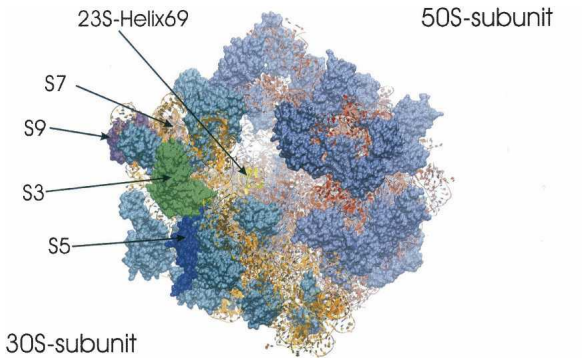

Figure 7. Diagram of the *E. coli* ribosome. VMD-generated representation of the *E. coli* ribosome with proteins shown as molecular surfaces (SURF plot, 1.4 Å) and RNA in ribbon format (Varshney et al. 1994; Humphrey et al. 1996). The 30S-subunit components discussed elsewhere in this text are highlighted as follows: S3 (green), S5 (navy blue), S7 (pink), S9 (purple), and 23S-Helix69 (yellow). All other proteins are shown in either cyan (30S subunit) or ice-blue (50S subunit), with 30S-RNA in orange and 50S-RNA in red.

The specific interaction of YhbZ with RluD, and ribosome structural proteins revealed by these studies is very interesting, and may be an example of a general mechanism whereby GTP-binding proteins and their partners are recruited and directed to the appropriate site on the ribosome. In this regard it is relevant to note that a eukaryotic GTPase, Bms1p, which is essential for small subunit production in *S. cerevisiae*, interacts with Rcl1p, a putative RNA modifying/cleavage protein. Rcl1p activates Bms1p through promoting GDP/GTP exchange in an event believed to be important for early stages in the small subunit assembly (Gelperin et al. 2001; Wegierski et al. 2001; Karbstein et al. 2005; Karbstein and Doudna 2006). These observations are consistent with GTPases having an evolutionarily conserved function that is to couple ribosome assembly and RNA modification/processing to their GTP-regulated activities.

Finally, as the EngA and YhbZ proteins have such a vital role in the biology of the prokaryotic ribosome, and consequently cell viability, they represent attractive targets for the development of antimicrobial compounds. Targeted inhibition of their GTPase-related functions can be achieved by developing compounds specific for their nucleotide-binding sites. The data shown in Figure 6A–C shows that a simple displacement assay can be used for high-throughput screening of compounds targeting the nucleotide-binding site. Inhibitors of this type may form the basis for the development of lead compounds with antimicrobial activity and a defined mode of action.

Materials and Methods

Gene cloning and recombinant protein purification

The DNA sequences encoding the EngA and YhbZ proteins were amplified from the *S. typhimurium* strain SL3261 by the PCR, subcloned into the vector pET3d using 5′ NcoI and 3′ BamHI sites (EngA and YhbZ), and their sequence determined to ensure that no mutations had occurred during the amplification process. DNA sequences encoding the S7, S9, RluD, and YegS proteins were synthesized by Blue Heron Biotechnology, and subcloned into the vector pET3a using NdeI and BamHI sites. The five recombinant plasmids generated by these procedures

were designated pMUT103 (YhbZ), pMUT106 (EngA), pMUT147 (S9), pMUT148 (S7), and pMUT151 (RluD). In order to facilitate purification by immobilized metal affinity chromatography (IMAC), the S7 and S9 proteins have additional 6H residues attached to their N terminus. The remaining three proteins are untagged, and thus of native amino acid sequence. For recombinant protein overproduction the plasmids were transformed into the *E. coli* expression strains BL21 DE3 (pMUT106), BL21 PlysS (pMUT103), or BL21 AI (pMUT147/8/151). Cells were grown with shaking (160 rpm) in 500 mL volumes in 2 L baffled Ehrlenmeyer flasks at 30°C in LB medium appropriately supplemented with antibiotics (100 μg mL^{-1} ampicillin and for PlysS additionally 35 μg mL^{-1} chloramphenicol) to an attenuance of 0.6. At this point recombinant protein overproduction was induced by the addition of IPTG to 0.2 mg mL^{-1} (DE3 and PlysS) or 0.2% (w/v) L-arabinose (BL21 AI). Induction was continued for a further 5 h at 30°C, at which point the cells were harvested by centrifugation and stored at −18°C until needed.

For S7 and S9 50 g of cell paste was sonicated in 500 mL 0.1 M Tris, 0.3 M NaCl pH 8.0, 1 mM benzamidine (buffer 1) while cooling in an ice-water bath. The sonicated cell suspensions were clarified by centrifugation at 10,000*g* for 42 min and loaded onto 250 mL Q Sepharose columns equilibrated previously with buffer 1. The columns were washed with 500 mL of 0.1 M Tris, 0.3 M NaCl pH 8.0 (buffer 2), and the column flow-through and wash were combined. For the S7 protein, the pool of protein was loaded onto a 50-mL IMAC column and washed with 500 mL of buffer 1. Bound proteins were eluted from the columns using 1L 0.0–0.3 M imidazole gradients in buffer 1, collecting 10 mL fractions. Desired proteins were identified by SDS-PAGE, pooled appropriately, and dialyzed against 2 × 5 L changes of 50 mM potassium phosphate pH 7.2, 1 mM DTT. 0.3 M NaCl (buffer 3). For the purification of S9, the post-Q Sepharose pool was dialyzed directly against buffer 2 without the IMAC step, as the S9 failed to bind to IMAC columns under any of the conditions tested. After dialysis, the proteins were further purified by FPLC on a MONO S 10/10 HR column equilibrated previously with buffer 2 in conjunction with an AKTA purification station. Bound proteins were eluted with a 20-column volume linear 0.3 M to 2.0 M NaCl gradient in buffer 3, collecting 2 mL fractions. Desired proteins were identified by SDS-PAGE and pooled appropriately, yielding ~35 mg S9 and 30 mg S7.

Cells (25 g) overproducing YhbZ were sonicated in 500 mL of 50 mM potassium phosphate pH 7.2, 1 mM DTT, 1 mM benzamidine (buffer 4) while cooling in an ice-water bath. The sonicated cell suspensions were clarified by centrifugation at 10,000*g* for 42 min and loaded onto a 250-mL Q Sepharose column equilibrated previously with buffer 3. The column was washed with 500 mL of 50 mM potassium phosphate pH 7.2, 1 mM DTT (buffer 5) and bound proteins eluted in 10 mL fractions with a 1-L 0.0–1.0 M NaCl gradient in buffer 5. Fractions containing YhbZ were identified by SDS-PAGE, pooled appropriately, and made 30% saturated with ammonium sulphate. The precipitate formed was recovered by centrifugation at 10,000*g* for 42 min, redissolved in 50 mL of buffer 5, and dialyzed against 2 × 5 L changes of buffer 5. The dialyzed pool was then applied to an ~140-mL hydroxyapatite column and the column washed with 500 mL of buffer 5. The column was eluted with a 1 L 50–400 mM potassium phosphate gradient (containing 1 mM DTT) collecting 10 mL fractions. YhbZ-containing fractions were identified by SDS-PAGE and pooled appropriately, typically yielding ~500 mg of purified YhbZ.

Cells (25 g) overproducing EngA were sonicated in 500 mL of 50 mM potassium phosphate pH 7.2, 1 mM DTT, 1 mM benzamidine (buffer 4) while cooling in an ice-water bath. The sonicated cell suspensions were clarified by centrifugation at 10,000*g* for 42 min and loaded onto a 250-mL Q Sepharose column equilibrated previously with buffer 5. The column was washed with 500 mL of buffer 5 and bound proteins eluted in 10 mL fractions with a 1-L 0.0–1.0 M NaCl gradient in buffer 5. Fractions containing EngA were identified by SDS-PAGE, pooled appropriately, and made 1.0 M with ammonium sulphate. This solution was then applied to a 250-mL phenyl Sepharose column equilibrated previously with 50 mM potassium phosphate pH 7.2, 1 mM DTT, 1.0 M NH_4SO_4 (buffer 6). The column was washed with 500 mL of buffer 6 and bound proteins eluted with a reverse linear gradient of 1.0 M to 0.0 M NH_4SO_4 in 50 mM potassium phosphate pH 7.2, 1 mM DTT, collecting 10-mL fractions. EngA-containing fractions were identified by SDS-PAGE, pooled appropriately, and dialyzed against 2 × 5 L changes of buffer 4. The dialyzed sample was loaded in halves onto two 125-mL hydroxyapatite columns and the sample washed through with 500 mL of buffer 4 collecting 10-mL fractions. EngA-containing fractions were identified by SDS-PAGE and pooled appropriately typically yielding ~800 mg of purified EngA.

RluD was purified by the same protocol as that for EngA, with the exception that RluD bound to the hydroxyapatite column and was eluted off with a 1-L 50–400-mM potassium phosphate gradient (containing 1 mM DTT) collecting 10-mL fractions. Typical yields of purified RluD were 700 mg from 25 g of cell paste. YegS was purified as described previously (Nichols et al. 2007).

The purification of a truncated *Thermus thermophilus* S7 protein lacking the sequence ARRRR (amino acids 2–6) has been reported previously, and shown to be facilitated by elevated levels of NaCl (Wimberly et al. 1997). As the production of large amounts of the *S. typhimurium* S7 and S9 proteins may have been partially toxic to *E. coli,* we chose to produce these proteins as 6His fusions so that we had the option of using IMAC as an affinity step if the proteins were poorly overproduced in *E. coli*. The purpose of using the complete sequence of S7 (i.e., including the sequence ARRRR deleted in other reports of S7 purification) was that, although the ARRRR sequence in S7 has been suggested as binding RNA (Wimberly et al. 1997), it is not known if it may, in addition, also contribute to protein:protein interactions. In order to purify S7 and S9 without contaminating nucleic acid, the overproducing strains of *E. coli* had to be sonicated in a buffer containing 0.3 M NaCl and the cell-free supernatants initially chromatographed on a MONO Q column. The MONO Q column bound the majority of the contaminating nucleic acid and the S7 and S9 proteins did not bind to the column. If this step was not taken, the S7 and S9 proteins at the end of the purification procedure had UV absorption spectra peaking at 260 nm. The high positive charge of both proteins (S7 ~+12 and S9 ~+16) was calculated by the Vector Nti suite of programs. This charge, together with the presence in S7 of a β-hairpin motif that binds double-stranded nucleic acids (Wimberly et al. 1997), is most likely the reason for their tight interactions with nucleic acid.

Isolation of partner proteins for YhbZ and EngA

A 1-L cell-free sonicated extract of 50 g of stationary phase *S. typhimurium* strain SL3261 in 50 mM potassium phosphate pH 7.2, 1 mM DTT, 1 mM benzamidine, 1 mM $MgCl_2$ (buffer 7) was incubated with 1000 Kunitz units of RNAse I with stirring

at room temperature for 1 h. The RNAse-treated sample was then loaded onto a 25 mL NHS-activated Sepharose column that had ~300 mg of YhbZ or EngA covalently attached to it. This and the following steps were all carried out at 5°C. The column was washed with 300 mL of buffer 4 and then eluted with a 500 mL 0–1.0 M NaCl gradient in buffer 2 collecting 5-mL fractions, and the entire elution profile was screened for protein by SDS-PAGE analysis.

Peptide mass fingerprinting

Approximately 0.2 μg of Coomassie Blue stained protein was excised from a 12% SDS-PAGE, subject to trypsin digestion and the peptides analyzed using an Applied Biosystems–DE STR instrument as described previously (Hellman et al. 1995).

Isothermal titration calorimetry

Isothermal titration calorimetry (ITC) is a nondestructive and noninvasive (label-free) technique that can be used to give a direct measure of the K_D and additionally provides information on the enthalpy (ΔH) and stoichiometry (n) of ligand binding. In these ITC experiments a protein solution is placed in a reaction vessel and ligands are titrated in from a syringe while constantly stirring the mixture. Any heat absorbed (endothermic reaction) or released (exothermic reaction) when ligand binds to the protein or two proteins interact is measured directly. Standard Gibbs free energy (ΔG^0) and entropy (ΔS^0) of ligand binding are subsequently calculated from the following equations:

$$\Delta G^0 = -RT \cdot \ln K_b = +\mathrm{RT} \cdot \ln K_D = \Delta H - \mathrm{T} \cdot \Delta S^0.$$

ITC experiments were performed at 25°C using a high precision VP-ITC system (Microcal Inc.). Proteins were dialyzed into 50 mM potassium phosphate pH 7.2, 1 mM DTT for interactions involving EngA, or 50 mM potassium phosphate pH 7.2, 1 mM DTT, 1 mM $MgCl_2$ for YhbZ. The concentrations of the various proteins and nucleotides used in the injector and cell are shown in Tables 2 and 3. The heat evolved following each 10-μL injection was obtained from the integral of the calorimetric signal. The heat due to the binding reaction was obtained as the difference between the heat of reaction and the corresponding heat of dilution. Analysis of data was performed using Microcal Origin software (Cooper and Johnson 1994; Cooper 1998).

BODIPY FL GDP binding

Measurements of BODIPY FL GDP fluorescence were performed with a Varian Eclipse fluorescence spectrophotometer with excitation at 488 nm and emission monitored at 512 nm. BODIPY FL GDP was diluted to a final concentration of 100 nM in 50 mM KPO_4 pH 7.2, 1 mM β-mercaptoethanol ± 1 mM Mg^{2+} and assays were carried out at 20°C. Direct titration of EngA was carried out by the addition of EngA in the concentration range of 0–5 μM and an increase in the fluorescence signal was observed. Competition assays to determine if GTP and GDP could displace the fluorescent analog were set up with 100 nM BODIPY FL GDP, 9 μM EngA in 50 mM KPO_4 pH 7.2, 1 mM β-mercaptoethanol ± 1 mM Mg^{2+}, and increasing concentrations of GTP or GDP. A decrease in the fluorescence emission intensity was observed with addition of GDP in the concentration range of 0–500 μM and for GTP in the concentration range of 0–4000 μM. Each experiment was carried out in triplicate, and the data points in Figure 6, showing the change in fluorescence intensity, are plotted with standard error bars using Origin 5 software (http://www.originlab.com). The K_D for BODIPY FL GDP binding to EngA was estimated by using a fit to a quadratic equation, while competitive binding curves were modeled by an iterative procedure using the Excel Solver routine.

M_r *determination of YhbZ*

The native M_r of YhbZ was investigated by size-exclusion chromatography using a Superdex 200 HR 10/30 column equilibrated with 50 mM KPO_4 pH 7.2, 150 mM NaCl, 1 mM DTT. Samples (1 mg) of YhbZ were chromatographed in triplicate and the native M_r estimated from a standard curve generated using standards of apoferritin (443 kDa), alcohol dehydrogenase (150 kDa), bovine serum albumin (66 kDa), carbonic anhydrase (29 kDa), and cytochrome *c* (12.4 kDa).

GTPase assay and thin-layer chromatograpy

The GTPase assay monitors the conversion of [γ-^{32}P]GTP to GDP by EngA or YhbZ. The reactions were carried out in 60-μL volume mixtures of 20 mM Tris HCl pH 7.5, 100 mM KCl, 5 mM $MgCl_2$, 0.15 mM THP, 0.5 mM GTP, with added trace amounts (<10 nM) [γ-^{32}P]GTP. For each protein the reaction was carried out in triplicate at concentrations of 0.5 μM and 1 μM for EngA and 1 μM and 2 μM for YhbZ. The samples were incubated at 30°C and 5-μL aliquots were removed at 20-min time intervals between 0 and 120 min, and the reaction was stopped with the addition of 1 μL 50 mM EDTA. The conversion of [γ-^{32}P]GTP to GDP was analyzed by thin-layer chromatography. A 2-μL portion of each sample was spotted onto a cellulose PEI polyester thin-layer chromatography plate (Fisher Scientific) and chromatographed in 0.5 M acetic acid, 0.5 M $LiCl_2$. Areas on the dried plates corresponding to [γ-^{32}P]GTP or GDP were quantified by measuring the relative pixel signal intensity using Fuji film phosphoimager BAS-1500 and Tina software version 2.09g (Raytest). The percentage conversion of GTP to GDP was plotted for each sample against time for each protein at the two separate concentrations, and for each protein the conversion was linear over time and dose dependent. A linear fit of data was carried out using Origin 5 software (http://www.originlab.com) and used to estimate the turnover number for each protein.

Assays to detect any enhancement of YhbZ GTPase activity by RluD were carried using 2 μM YhbZ in the standard reaction mixture and samples were set up with increasing levels of RluD in the concentration range of 0–10 μM. A control experiment was carried out in parallel with 2 μM YhbZ and increasing concentrations of BSA in the concentration range of 0–10 μM. The samples were incubated at 30°C for 1 h and analyzed at each RluD and BSA concentration for the conversion of [γ-^{32}P]GTP to GDP as described above.

Acknowledgments

Financial support was received from Arrow Therapeutics and the United Kingdom Biotechnology and Biological Sciences Research Committee LINK program.

Competing interests statement

A.R.H., I.G.C., and D.K.S. are cofounders of Arrow Therapeutics, and A.R.H. and D.K.S. are consultants to the company.

References

Bharat, A., Jiang, M., Sullivan, S.M., Maddock, J.R., and Brown, E.D. 2006. Cooperative and critical roles for both G domains in the GTPase activity and cellular function of ribosome-associated *Escherichia coli* EngA. *J. Bacteriol.* **188:** 7992–7996.

Brown, E.D. 2005. Conserved P-loop GTPases of unknown function in bacteria: An emerging and vital ensemble in bacterial physiology. *Biochem. Cell Biol.* **83:** 738–746.

Buglino, J., Shen, V., Hakimian, P., and Lima, C.D. 2002. Structural and biochemical analysis of the Obg GTP-binding protein. *Structure* **10:** 1581–1592.

Butland, G., Peregrin-Alvarez, J.M., Li, J., Yang, W., Yang, X., Canadien, V., Starostine, A., Richards, D., Beattie, B., Krogan, N., et al. 2005. Interaction network containing conserved and essential protein complexes in *Escherichia coli*. *Nature* **433:** 531–537.

Caldon, C.E. and March, P.E. 2003. Function of the universally conserved bacterial GTPases. *Curr. Opin. Microbiol.* **6:** 135–139.

Caldon, C.E., Yoong, P., and March, P.E. 2001. Evolution of a molecular switch: Universal bacterial GTPases regulate ribosome function. *Mol. Microbiol.* **41:** 289–297.

Comartin, D.J. and Brown, E.D. 2006. Non-ribosomal factors in ribosome subunit assembly are emerging targets for new antibacterial drugs. *Curr. Opin. Pharmacol.* **6:** 1–6.

Cooper, A. 1998. Microcalorimetry of protein–protein interactions. *Methods Mol. Biol.* **88:** 11–22.

Cooper, A. and Johnson, C.M. 1994. Isothermal titration microcalorimetry. *Methods Mol. Biol.* **22:** 137–150.

Dutca, L.M. and Culver, G.M. 2005. Regulation of rRNA processing: A role for a unique GTPase. *Mol. Cell* **20:** 497–499.

Gelperin, D., Horton, L., Beckman, J., Hensold, J., and Lemmon, S.K. 2001. Bms1p, a novel GTP-binding protein, and the related Tsr1p are required for distinct steps of 40S ribosome biogenesis in yeast. *RNA* **7:** 1268–1283.

Gutgsell, N.S., Deutscher, M.P., and Ofengand, J. 2005. The pseudouridine synthase RluD is required for normal ribosome assembly and function in *Escherichia coli*. *RNA* **11:** 1141–1152.

Hellman, U., Wernstedt, C., Gonez, J., and Heldin, C.H. 1995. Improvement of an ''In-Gel'' digestion procedure for the micropreparation of internal protein fragments for amino acid sequencing. *Anal. Biochem.* **224:** 451–455.

Humphrey, W., Dalke, A., and Schulten, K. 1996. VMD: Visual molecular dynamics. *J. Mol. Graph.* **14:** 27–38.

Hwang, J. and Inouye, M. 2001. An essential GTPase, Der, containing double GTP-binding domains from *Escherichia coli* and *Thermotoga maritima*. *J. Biol. Chem.* **276:** 31415–31421.

Hwang, J. and Inouye, M. 2006. The tandem GTPase, Der, is essential for the biogenesis of 50S ribosomal subunits in *Escherichia coli*. *Mol. Microbiol.* **61:** 1660–1672.

Jiang, M., Datta, K., Walker, A., Strahler, J., Bagamasbad, P., Andrews, P.C., and Maddock, J.R. 2006. The *Escherichia coli* GTPase CgtAE is involved in late steps of large ribosome assembly. *J. Bacteriol.* **188:** 6757–6770.

Karbstein, K. and Doudna, J.A. 2006. GTP-dependent formation of a ribonucleoprotein subcomplex required for ribosome biogenesis. *J. Mol. Biol.* **356:** 432–443.

Karbstein, K., Jonas, S., and Doudna, J.A. 2005. An essential GTPase promotes assembly of preribosomal RNA processing complexes. *Mol. Cell* **20:** 633–643.

Knuth, K., Niesalla, H., Hueck, C.J., and Fuchs, T.M. 2004. Large-scale identification of essential *Salmonella* genes by trapping lethal insertions. *Mol. Microbiol.* **51:** 1729–1744.

Liiv, A., Karitkina, D., Maivali, U., and Remme, J. 2005. Analysis of the function of *E. coli* 23S rRNA helix-loop 69 by mutagenesis. *BMC Mol. Biol.* **6:** 18. doi: 10.1186/1471-2199-6-18.

Misra, R.V., Horler, R.S., Reindl, W., Goryanin, I.I., and Thomas, G.H. 2005. EchoBASE: An integrated post-genomic database for *Escherichia coli*. *Nucleic Acids Res.* **33:** D329–D333. doi: 10.1093/nar/gki028.

Muench, S.P., Xu, L., Sedelnikova, S.E., and Rice, D.W. 2006. The essential GTPase YphC displays a major domain rearrangement associated with nucleotide binding. *Proc. Natl. Acad. Sci.* **103:** 12359–12364.

Nichols, C.E., Lamb, H.K., Lockyer, M., Charles, I.G., Pyne, S., Hawkins, A.R., and Stammers, D.K. 2007. Characterization of *Salmonella typhimurium* YegS, a putative lipid kinase homologous to eukaryotic sphingosine and diacylglycerol kinases. *Proteins* **68:** 13–25.

O'Brien, J., Ladbury, J.E., and Chowdry, B.Z. 2000. Isothermal titration calorimetry of biomolecules. In *Protein–ligand interactions: Hydrodynamics and calorimetry* (eds. S.E. Harding and B.Z. Chowdry), pp. 263–286. Oxford University Press, Oxford, UK.

Poehlsgaard, J. and Douthwaite, S. 2005. The bacterial ribosome as a target for antibiotics. *Nat. Rev. Microbiol.* **3:** 870–881.

Robinson, V.L., Hwang, J., Fox, E., Inouye, M., and Stock, A.M. 2002. Domain arrangement of Der, a switch protein containing two GTPase domains. *Structure* **10:** 1649–1658.

Sato, A., Kobayashi, G., Hayashi, H., Yoshida, H., Wada, A., Maeda, M., Hiraga, S., Takeyasu, K., and Wada, C. 2005. The GTP binding protein Obg homolog ObgE is involved in ribosome maturation. *Genes Cells* **10:** 393–408.

Schuwirth, B.S., Borovinskaya, M.A., Hau, C.W., Zhang, W., Vila-Sanjurjo, A., Holton, J.M., and Cate, J.H. 2005. Structures of the bacterial ribosome at 3.5 Å resolution. *Science* **310:** 827–834.

Spedaliere, C.J., Ginter, J.M., Johnston, M.V., and Mueller, E.G. 2004. The pseudouridine synthases: Revisiting a mechanism that seemed settled. *J. Am. Chem. Soc.* **126:** 12758–12759.

Sullivan, S.M., Mishra, R., Neubig, R.R., and Maddock, J.R. 2000. Analysis of guanine nucleotide binding and exchange kinetics of the *Escherichia coli* GTPase era. *J. Bacteriol.* **182:** 3460–3466.

Tan, J., Jakob, U., and Bardwell, J.C. 2002. Overexpression of two different GTPases rescues a null mutation in a heat-induced rRNA methyltransferase. *J. Bacteriol.* **184:** 2692–2698.

Varshney, A., Brooks, F., and Wright, W. 1994. Linearly scalable computation of smooth molecular surfaces. *IEEE Comp. Graph. Appl.* **14:** 19–25.

Wegierski, T., Billy, E., Nasr, F., and Filipowicz, W. 2001. Bms1p, a G-domain-containing protein, associates with Rcl1p and is required for 18S rRNA biogenesis in yeast. *RNA* **7:** 1254–1267.

Welsh, K.M., Trach, K.A., Folger, C., and Hoch, J.A. 1994. Biochemical characterization of the essential GTP-binding protein Obg of *Bacillus subtilis*. *J. Bacteriol.* **176:** 7161–7168.

Wimberly, B.T., White, S.W., and Ramakrishnan, V. 1997. The structure of ribosomal protein S7 at 1.9 A resolution reveals a β-hairpin motif that binds double-stranded nucleic acids. *Structure* **5:** 1187–1198.

Wimberly, B.T., Brodersen, D.E., Clemons Jr., W.M., Morgan-Warren, R.J., Carter, A.P., Vonrhein, C., Hartsch, T., and Ramakrishnan, V. 2000. Structure of the 30S ribosomal subunit. *Nature* **407:** 327–339.

Wiseman, T., Williston, S., Brandts, J.F., and Lin, L.N. 1989. Rapid measurement of binding constants and heats of binding using a new titration calorimeter. *Anal. Biochem.* **179:** 131–137.

Wittinghofer, A. 2002. Obg, a G domain with a beautiful extension. *Structure* **10:** 1471–1472.

Wout, P., Pu, K., Sullivan, S.M., Reese, V., Zhou, S., Lin, B., and Maddock, J.R. 2004. The *Escherichia coli* GTPase CgtAE cofractionates with the 50S ribosomal subunit and interacts with SpoT, a ppGpp synthetase/hydrolase. *J. Bacteriol.* **186:** 5249–5257.